# Increased stromal densities of B cells, CD103+ cells, and CD163+ M2-like macrophages associate with poor clinical outcomes in BCG treated non-muscle invasive bladder cancer

Benjamin Ravenscroft[1], Priyanka Yolmo[2,3], Stephen Chenard[2,3], Sadaf Rahimi[2,3], Keiran Pace[2, 3], Kartik Sachdeva[2,3], Tamara Jamaspishvilli[1], Hamid Ghaedi[1,3], Andrew Garven[1,3], Kathrin Tyryshkin[1,3], David M. Berman[1,3], Chelsea Jackson[1,4], D. Robert Siemens[3,5], Madhuri Koti*[2, 3]

[1]Pathology and Molecular Medicine, Queen's University, Kingston, ON, Canada;[2]Department of Biomedical and Molecular Sciences, Queen's University, Kingston, ON, Canada; [3]Cancer Research Institute, Queen's University, Kingston, ON, Canada; [4]Department of Pathology, University of Manitoba; [5]Department of Urology, Queen's University, Kingston, ON, Canada.

**Key words:** B cells, NMIBC, BCG immunotherapy

***To whom correspondence should be addressed**

e-mail: kotim@queensu.ca

**Abstract**

Non-muscle invasive bladder cancer (NMIBC) constitutes a significant clinical challenge, with over 50% of patients experiencing poor clinical outcomes in the form of early recurrence or progression following treatment with Bacillus Calmette-Guerin (BCG) immunotherapy. The pre-treatment tumor immune microenvironment (TIME) is an established determinant of response to BCG. This study explores the spatial profiles of CD79a+ B cells, CD163+ M2-like macrophages, proliferating and tissue-resident phenotypes of T cells, along with PD-1/PD-L1 checkpoint expression in pre-BCG treatment tumors of 173 patients (139 males, 34 females). Multiplex immunofluorescence staining of a tumor tissue microarray, revealed elevated infiltration of CD79a+ B cells, CD163+ M2-like macrophages, CD103+ cells, and CD8+ T cells at the tumor invasive margins. Increased epithelial PD-L1 immune-checkpoint expression in tumors was observed in female and male patients who exhibited significantly shorter recurrence-free survival (RFS). Importantly, high CD79a+ B cell density in BCG-treated females in both stromal and epithelial compartments exhibited significantly shorter RFS and progression-free survival compared to males. Stromal CD79a+ B cell density was positively correlated with M2-like macrophages, CD8+ T cells, CD103+ cells and PD-1 expressing cells. CD79a+ B cells, CD103+ cells, and M2-like macrophage density were associated with higher grade and enriched in basal subtype tumor. This study highlights the significance of an understudied role of B cells and their cellular neighborhoods in the pre-treatment TIME and BCG-therapy response. Overall, findings from this study underscore the importance of considering sex-related immunobiological differences in the stromal compartments of bladder tumors towards the development of optimal therapeutic targeting strategies.

42 **Introduction**

43 Approximately 75% of newly diagnosed bladder cancer patients present with NMIBC. While the
44 incidence of NMIBC is four times higher in males, female patients with NMIBC often present
45 with a more advanced stage and display earlier recurrence [1-4]. Patient age, tobacco smoking,
46 and occupational exposure to chemicals are some of the major risk factors associated with
47 NMIBC [5-7]. Bacillus Calmette-Guérin (BCG), a live attenuated strain of *Mycobacterium bovis*,
48 is the adjuvant treatment for patients with intermediate or high-risk NMIBC [8, 9]. Intravesical
49 BCG therapy entails 6 weekly instillations after transurethral resection of bladder tumor
50 (TURBT), followed by a maintenance schedule of 3 weekly instillations every 3-6 months for 1-3
51 years depending on the risk stratification as defined by the American and European Urological
52 Association [9]. Despite its proven efficacy, over 50% of the patients receiving BCG
53 immunotherapy experience recurrence or become unresponsive to treatment [5, 6]. Second
54 line treatments such as programmed cell death protein-1 receptor/ligand (PD-1/PD-L1) immune
55 checkpoint axis inhibitors and replication deficient adeno viral gene-delivery vectors
56 (Adstiladrin) are under trials for BCG unresponsive/recurrent disease [10-12]. While some have
57 demonstrated modest benefits, these newer treatment approaches do not increase primary
58 response to BCG and are not indicated in the BCG naïve setting [13-15].

59 The pre-treatment TIME is a major determinant of response to immunotherapy across various
60 cancers [11, 16, 17]. Recent studies have established that the pre-treatment TIME plays an
61 important role in determining BCG therapy response in patients with NMIBC [18-21]. This is
62 especially important when considering BCG therapy, which involves a live bacterial preparation
63 and its efficacy is dependent on multiple factors including the dose, viability of bacteria at the
64 time of instillation, immune physiological status of the host, bacterial contact with the
65 urothelium and uptake by cells in the bladder mucosal immune environment. Based on the
66 infiltration profiles of CD8+ cytotoxic T cells, FoxP3+ $T_{reg}$ cells, and the expression patterns of
67 PD-1/PD-L1+ immune checkpoints, both in pre-BCG treatment and recurrent tumors, a
68 potential role of adaptive immune resistance has also been suggested [19]. Additionally,
69 elevated T cell exhaustion has been reported as a major factor underlying poor response to BCG
70 [20]. In our previous report, conducted on the whole transcriptomic profiles of the UROMOL

71 cohort (n=460) and spatial immunophenotyping of tumors from a large cohort assembled at the
72 Kingston Health Sciences Center (KHSC, n=332), we showed increased infiltration of B cells, M2-
73 like macrophages, and higher expression of PD-L1 in the pre-treatment TIME of both female
74 and male patients experiencing early recurrence, irrespective of the treatment type [18].
75 Notably, female patients with high-grade disease in both cohorts exhibited significantly shorter
76 progression free survival (PFS) and had higher infiltration of B cells and M2-like macrophages in
77 their pre-treatment tumors compared to their male counterparts. In the current study, we
78 characterized the association between immune cell spatial profiles in the BCG-naïve TURBT
79 specimens of female and male patients exhibiting differential response to BCG immunotherapy,
80 from our previously reported KHSC cohort [18]. Given the established differences in sex-
81 associated B cell immunobiology and the need for improved patient stratification for increased
82 benefits from BCG immunotherapy, we further evaluated patient sex-associated pre-BCG tumor
83 immune profiles and clinical outcomes.

84

85 **METHODS**

86 **Ethics statement**

87 This study was approved by the Queen's University Health Sciences and Affiliated Teaching
88 Hospitals Research Ethics Board.

89

90 ***In silico* analysis of *CD79A, CD103* and *CD163* gene expression profiles in transcriptomic**
91 **profiles of tumors from BCG naïve high-risk patients**

92 Based on our previous findings [18] on the associations between tumor infiltrating CD79a+ B
93 cells and M2-like macrophage densities and overall poor clinical outcomes in patients with
94 NMIBC, irrespective of the treatment type, we first evaluated the publicly available normalized
95 bulk RNA-sequencing based tumor whole transcriptome profiles of 283 patients with NMIBC
96 that was recently generated by Jong *et al.,* [21]. The patients in this cohort were stratified into
97 different quartiles according to their *CD79a* and *CD163* gene expression levels. Patient clinical

98 demographics and outcome data was extracted from the supplementary information provided
99 by de Jong *et al.*, [21] These clinical attributes were then combined with the gene expression
100 profiles of the primary tumors. Subsequently, an analysis was conducted using the time to
101 disease progression and the progression status in R version 4.2.0. To visualize the relationship
102 between target *gene* expression and survival, Kaplan-Meier survival curves were generated by
103 employing a log-rank statistical analysis method and utilizing the survival and survminer
104 packages in R.

105

106 **KHSC-BCG Patient Cohort and Clinical Data**

107 Given their critical roles in mucosal immunobiology we then asked whether the spatial profiles
108 of CD79a+ B cells, CD163+ M2-like macrophages and other immune cells of interest (see below)
109 associate with variable response to BCG in female and male patients with NMIBC. Of the 332
110 patients reported in our previous study [18], a total of 173 patients (KHSC-BCG:139 males and
111 34 females) who received at least one induction round of BCG, defined as at least 5/6
112 instillations, and had no BCG treatment prior to entering the cohort, were selected for inclusion
113 in this study (**Table 1**). Adequate BCG treatment was defined as an initial induction round of at
114 least 5/6 instillations, followed by a maintenance round of at least 2/3 instillations [9]. Patients
115 were assessed for BCG therapy response and classified as either BCG refractory, BCG
116 responders, or an in-between state of therapy response. The BCG refractory state was defined
117 according to the recent consensus guidelines put forth by the European Association of Urology
118 [6], and BCG responders were patients without any high-grade recurrence within the two years,
119 following their first adequate BCG induction (**Table 1**)[8]. Due to our cohort size limitations and
120 the differences in clinical treatment versus ideal clinical trial treatment pathways, we used high-
121 grade recurrence as an endpoint for time-to-event analysis. The initiation point for time-to-
122 event analyses is the diagnosis of TURBT immediately prior to the initiation of BCG treatment.
123 Progression events were defined as recurrence to stage T2 or higher.

124 Baseline clinical data and NMIBC tissue were collected for eligible patients (**Table 2**). All the
125 tumor tissue specimens included in the study were index TURBT specimens. The median follow-

126 up from surgical resection (TURBT) was 54.3 months (95% CI 50.2 to 59.5 months) for the
127 cohort. 124 (71.7%) of the cohort were BCG responders and 37 (21.4%) were BCG refractory.
128 The entire cohort had a 24-month high-grade recurrence free survival (RFS) rate of 70% (95% CI
129 63.1% to 77.5%). The median time to HG recurrence was 7.6 months (95% CI 6.3 to 11.8
130 months), and the median follow-up time for BCG responders was 53.4 months (95% CI 47.8 to
131 59.5 months).

132

133 **Multiplex Immunofluorescence Staining**

134 Three panels of antibodies were used to stain the tissue microarrays (TMAs; **Supplementary**
135 **data, Figure S1**). The first panel consisted of antibodies identifying FoxP3+, CD8+, CD3+, and
136 Ki67+ cells. The second panel PD-1+, PD-L1+, and CK5+ cells and the third panel included
137 antibodies identifying GATA3+, CD103+, CD163+, and CD79a+ cells. The following cell types
138 were evaluated for expression in both the epithelium and stroma: proliferating and non-
139 proliferating cytotoxic T cells (CD3+CD8+Ki67+/-), cytotoxic regulatory and non-regulatory T
140 cells (CD3+FoxP3+/-), immune checkpoints (PD-1+, PD-L1+, PD-L1+ expressed on CK5+ cancer
141 cells and immune cells), CD103+ cells, CD163+ M2-like macrophages and CD79a+ B cells.
142 Staining and scanning of the TMA was performed using multiplex immunofluorescence (mIF)
143 staining at the Molecular and Cellular Immunology Core (MCIC) facility, BC Cancer Agency as
144 described earlier [18]. The antibodies utilized were supplied by Biocare Medical (Pacheco, CA,
145 USA) and distributed by Inter Medico (Markham, ON, CAN).

146

147 **Automated scoring and manual validation of immune cell density and distribution in mIF**
148 **stained tumors**

149 The stained TMA sections were scanned using the Vectra 3.0.5 multispectral imaging system
150 (PerkinElmer, MA, USA) and subsequently analyzed in InForm 2.4.0 (PerkinElmer, MA, USA).
151 The scanned TMAs underwent tissue segmentation into epithelium and stroma utilizing
152 InForm's tissue segmentation algorithm, specifically examining nuclear DAPI. Phenotyping was

153 performed by training three independent algorithms on ten randomly selected cores from the
154 cohort. The software identified positive pixels for all selected immune markers using each of
155 the three independent algorithms. The average was taken across the three algorithms for all
156 three sets of immune markers in each core. Cores containing ≤ 25% of the tissue were excluded
157 from subsequent analyses. Standard deviation between the three algorithms was calculated for
158 each of the immune markers within both the epithelial and stromal compartments. Outliers
159 were identified and cross-referenced with the composite image of the corresponding TMA core
160 to verify the discrepancy before excluding the outlying data points from further analysis. Any
161 quantifications that included misidentification of histological artifacts as immune cells by any of
162 the three algorithms were also excluded from analysis. Algorithms that consistently over-called
163 or under-called the immune marker quantification were excluded from analysis. Further visual
164 validation of the automated scoring was performed for randomly selected TMA cores.

165

166 **Statistical Analysis**

167 All analyses were conducted using either R version 4.1.2 or Python 3.9.12. Analysis of cell
168 population composition was performed using unpaired non-parametric Mann-Whitney tests.
169 The corrplot package was utilized to calculate and visualize the Spearman rank correlations of
170 various cell type, due to its non-parametric nature making it better suited for data lacking
171 normality. The Kaplan-Meier method and log-rank test were performed to determine the
172 association between time to high-grade recurrence and dichotomized infiltration of immune
173 cell phenotypes.

174 Differences in infiltration levels of immune cells between BCG refractory patients and BCG
175 responders were tested and presented with violin plots. Prior to statistical analysis, the
176 normality condition was checked for the density of each phenotype across the whole cohort
177 using the Shapiro-Wilk test. Failing to satisfy this condition, the Wilcox-rank sum test was used
178 to test for differences in immune cell infiltration in BCG responders and non-responders as it
179 does not assume normality.

180 To dichotomize infiltration of specific immune cell phenotypes, a combination of graphical
181 diagnostic plot methods as presented by Williams *et al.* and bootstrapping were used
182 (Microsoft Word - Technical report 79 cover mandrekar 6-06.doc (mayo.edu). Unique densities
183 of each immune phenotype were used to create indicator variables that could fit Cox models,
184 from which log-likelihood values could be extracted. These values were plotted, and LOESS
185 curve fitting was performed using the stats package. The discrete infiltration values closest to
186 the five most visually unique peaks were selected. Bootstrapping was performed using a
187 univariable cox model that compared the high/low infiltration groups for each of the six
188 possible cut point values previously identified [18]. The validated cut point was the
189 dichotomization value with the greatest frequency of maximum log-likelihood after
190 bootstrapping. Valid cut points were used to create dichotomized Kaplan-Meier curves
191 comparing RFS and PFS between high and low infiltration groups for various immune cell
192 phenotypes. The dichotomized Kaplan-Meier curves were typically truncated prior to the
193 number at risk in any group dropping below 5.

194 The distribution of clinically prognostic variables previously evaluated [18], including subtype,
195 grade, stage, AUA risk score, sex, and age, was rigorously examined for each dichotomized
196 immune cell phenotype. Statistical analysis involved employing Pearson's $\chi^2$ test or Fisher's
197 Exact test in cases where all assumptions were not met. P-values were calculated both without
198 adjustment for multiple testing and with adjustment for multiple testing using the Bonferroni
199 method.

200 The clinical impact of immune cell and immune checkpoint populations were analyzed using a
201 univariable Cox proportional hazards (CPH) model. The proportional hazards (PH) assumption
202 was verified using the Schoenfeld test, computed using the survival package. A nonsignificant ($p$
203 $> 0.05$) test statistic indicates that the PH assumption is met. Multivariable models were
204 created for each immune cell phenotype with age, sex, AUA risk score, and BCG treatment
205 amount, dichotomized into induction only and adequate BCG treatment groups, as covariates.
206 P-values were calculated with and without adjusting for multiple testing using the Bonferroni
207 method for correction of multiple testing. Results are reported graphically in a forest plot and
208 hazard ratios (HR) for immune cell density variables are scaled by the one standard deviation of

209 the given immune cell population when graphically reported. Scaling the hazard ratios by each
210 immune cell population's standard deviation in the cohort was performed to enable clearer
211 understanding of relative association between each cell type and RFS/PFS, as well as
212 comparison of each different cell type's effect size. Some cell types have a very low SD in the
213 cohort, such as stromal CK5+PD-L1+ (SD = 5.06), while others, such as stromal CD79a+ B cells
214 (SD = 137.13), have a very large standard deviation. Subsequently, reporting HR scaled by SD
215 (hereafter denoted $HR_{SD}$) shows effect size relative to expected magnitude of change in cell
216 infiltration for a given cell type [22].

217

218 **RESULTS**

219 ***Increased expression of CD79A and CD163 genes in pre-treatment tumors is associated with***
220 ***shorter progression free survival following treatment with BCG***

221 We first determined the association between expression levels of *CD79A* and *CD163* transcripts
222 and clinical outcomes using the publicly available and recently published large independent
223 cohort of BCG treated patients [21]. In this cohort of 283 patients, 20% of the patients were
224 female and the entire cohort was BCG-naive high-risk NMIBC with 34% of the patients
225 exhibiting progression after treatment with BCG. Kaplan-Meier survival analysis revealed that
226 high expression of *CD79A and CD163 are* associated with significantly shorter PFS following BCG
227 therapy (**Supplementary data, Figure S2**). In this cohort, this association was observed in both
228 male and female patients (not shown).

229

230 ***High CD79a+ B cell infiltration in stromal and epithelial regions is associated with early***
231 ***recurrence and progression following BCG therapy***

232 The patient clinical demographics of KHSC-BCG cohort are presented in **Table 2**. Of the 173
233 patients in the KHSC-BCG cohort, 72% patients had a diagnosis of high-grade disease. The
234 cohort reflected a female to male ratio of 1:4. Approximately 47% of patients in this cohort
235 received adequate BCG and risk stratification was performed as per the recent IBCG guidelines

236 (**Supplementary data, Figure S3**). High-grade recurrence was observed in 33% patients in this
237 cohort with 37 patients classified as BCG refractory and 124 as BCG responders. In this study,
238 we used CD79a as the pan B cell marker. Kaplan-Meier survival analysis revealed that both
239 female and male patients with high epithelial and stromal CD79a+ B cells in their pre-treatment
240 tumors had significantly shorter RFS and PFS (**Figure 1A, 1B** and **S4**). Furthermore, comparison
241 of the survival profiles specific to male and female patients revealed that females with high
242 stromal density of CD79a+ B cells in their pre-BCG tumors experienced worse RFS and PFS
243 (**Supplementary data, Figure S5**) compared to males. Quantification of immune cells in the
244 stromal regions showed a significantly higher density of CD79a+ B cells (p=0.015) and CD163+
245 M2 macrophages (p=0.027) in BCG refractory patients compared to the responders (**Figure 1C**
246 **and 1D**). Similar analysis of CD163+ cell densities within the epithelial compartment did not
247 show any significant differences (**Supplementary data, Figure S6**).

248

249 ***Stromal CD79a+ B cell density is positively correlated with M2-like macrophages, CD8+***
250 ***cytotoxic T cells, CD103+ cells and PD-1 immune checkpoint expression***

251 We then evaluated the correlations between cell types and immune checkpoint expression in
252 both the stromal and epithelial compartments. Spearman correlation analysis revealed
253 significantly positive correlations between CD79a+ B cells and CD163+ M2-like macrophages
254 (r=0.74, $p=1x10^{-7}$), CD3+ CD8+ cytotoxic T cell (r=0.55, $p=4x10^{-4}$), and PD-1 immune checkpoint
255 expressing cells (r=0.55, $p=4x10^{-4}$) in the stromal compartment of the BCG refractory group
256 (**Figure 2A**). Similar correlations were observed in the BCG responder group in which CD79a+ B
257 cells were significantly positively correlated with CD163+ M2 macrophages (r=0.61, $p=3x10^{-14}$),
258 CD3+CD8+ cytotoxic T cells (r=0.68, $p=2x10^{-10}$), and both PD-1 (r=0.67, $p=2x10^{-16}$) and PD-L1
259 (r=0.54, $p=7x10^{-11}$) immune checkpoints (**Figure 2B**). Importantly, within the BCG refractory
260 group, correlations between immune cell types in the epithelial compartments were not
261 significant as observed within the stromal region (**Figures 2C and 2D**). In the stromal regions of
262 tumors from BCG responder and refractory groups, CD163+ macrophages and CD8+ cytotoxic T
263 cells also depicted moderate positive correlation with each other (r=0.67-0.68). Cytotoxic T cell

density was highly correlated with the expression of PD-1 immune checkpoint (r=0.87-0.88) in both the groups.

***Increased stromal density of CD8+ T cells, CD103+ cells and M2-like macrophages is associated with early recurrence post-BCG***

Investigation of other immune cells in the stromal and epithelial compartment of each tumor core demonstrated a higher density of CD163+ M2-like macrophages, CD3+CD8+ cytotoxic T cells, and CD103+ cells in the BCG non-responder group. Kaplan-Meier survival analysis revealed a significant association between high stromal density of immune cells (M2-like macrophages, cytotoxic T cells and CD103+ cells) and overall shorter RFS (HR=2.87, $p < 0.001$, **Figure 3**).

Spearman correlation analysis revealed that PD-1+ cell density is highly and significantly correlated with CD103+ (r=0.64-0.83), CD163+ M2-like macrophages (r=0.62-0.65), and both Ki67+ and Ki67- CD8+ T cells (r=0.8-0.85). Furthermore, significant correlations were observed between PD-1 and CD103+ cells (r=0.64-0.83), in the stromal compartment indicate heightened immune checkpoint expression in these cells. Similarly, a strong correlation (**Figure 2A and 2B**) was found between PD-1 expression and both proliferating (Ki67+) and non-proliferating (Ki67-) cytotoxic CD8 + T cells (r=0.8-0.85). High expression of PD-1 could potentially suggest T cell activation in BCG responders and a state of immune exhaustion in BCG refractory patients. These findings underscore the considerable variability in immune responses to BCG immunotherapy.

***Elevated density of stromal CD79a+ B cells, CD8+ T cells, CD103+ cells, and M2-like macrophages is associated with increased disease stage and heightened AUA risk score***

To determine the stage and risk associated immune cell profiles, we performed a Pearson's $\chi^2$ analysis (**Supplementary data**, **Table S1**). Among the patients who received BCG treatment, a higher density of CD79a+ B cells, CD103+ cells, and M2-like macrophages in the stromal compartment of their tumors was associated with higher grade ($\chi^2(1, N=173) = 10.23$, $p = 0.001$,

292 $\chi^2(1, N=173) = 5.54$, $p = 0.019$, $\chi^2(1, N=173) = 5.95$, $p = 0.015$, respectively) and stage ($\chi^2(1,$
293 $N=173) = 6.11$, $p = 0.013$, $\chi^2(1, N=173) = 9.55$, $p = 0.002$, respectively), except for the higher
294 CD79+ B cell density. The basal subtype was notably more prevalent in patients with an
295 elevated stromal density of CD79a+ B cells and CD103+ cells, as confirmed by a Fisher's Exact
296 test (p = 0.016 and 0.025, respectively).
297
298 ***Univariable and multivariable analysis reveals high pre-BCG tumor immune cell density is***
299 ***associated with a higher risk of recurrence and progression***
300 A CPH based analysis revealed significant associations between immune cell infiltration profiles
301 and clinical outcomes (**Figure 4**). Specifically, in the epithelium PD-1+ ($HR_{SD}$=1.223, p=0.026),
302 CD79a+ B cells ($HR_{SD}$=1.198, p=0.024), and CK5+ PD-L1+ cancer ($HR_{SD}$=1.241, p=0.019) cell
303 density was associated with worse RFS (**Supplementary data Table S2**). CD79a+ B cells
304 ($HR_{SD}$=1.324, p=0.022), CD163+ M2-like macrophages ($HR_{SD}$=1.578, $p < 0.001$), CK5+PD-L1+
305 cancer cells ($HR_{SD}$=1.391, p=0.01), and PD-1+ immune checkpoint expressing cells ($HR_{SD}$=1.352,
306 p=0.017), in the epithelial compartment, were also associated with worse PFS (**Supplementary**
307 **data Table S3**).
308 In the stroma, CD3+CD8+ cytotoxic T cells ($HR_{SD}$=1.258, p=0.008), CD79a+ B cells ($HR_{SD}$=1.315, p
309 $< 0.001$), CD163+ M2-like macrophages ($HR_{SD}$=1.274, p=0.009), CD103+ cells ($HR_{SD}$=1.322,
310 p=0.014), and PD-1+ immune checkpoint expressing cells ($HR_{SD}$=1.415, p=0.006) were
311 associated with worse RFS. Only CD79a+ B cells ($HR_{SD}$=1.508, p=0.002), and CD163+ M2-like
312 macrophages ($HR_{SD}$=1.438, p=0.029), in the stromal compartment, were significantly associated
313 with PFS.
314 In a multivariable model considering sex, age, AUA risk score, and BCG treatment adequacy as
315 covariates, none of the immune cells in either the stromal or epithelial compartment were
316 significantly associated with a change in RFS after adjustment for multiple hypothesis testing.
317 CD79a+ B cells, in the stromal compartment, were however significantly associated with worse
318 PFS ($HR_{SD}$=1.663, p=0.03), with and without Bonferroni correction.
319
320

321 **Discussion**

322 Recurrence or progression to muscle invasive disease following BCG immunotherapy remain
323 the major challenges in the management of patients with NMIBC. To determine the factors that
324 lead to a poor response, studies have extensively examined the treatment-naïve TIME in
325 tumors collected at TURBT from patients with NMIBC. Specifically, these prior investigations
326 have focused on T cells and myeloid cells and have significantly advanced the current state of
327 knowledge on the complex nature of the TIME in NMIBC tumors [19, 20, 23, 24]. However,
328 clinical translation to actionable biomarkers is still unavailable. Additionally, B cells that
329 constitute the key cellular mediators of mucosal immunity, via their dual functions as antigen
330 presenting and antibody producing cells, remain understudied in the context of response to
331 BCG immunotherapy.

332 A significant and novel observation from the current study is the association between a high
333 density of stromal and intra-epithelial B cells in the BCG naïve tumors from patients who
334 experienced early recurrence or progression to muscle invasive disease. Our findings
335 demonstrate a robust association between CD79a+ B cell infiltration in both stromal and
336 epithelial compartments, which is more pronounced in high-grade tumors from female patients
337 who experienced early recurrence and disease progression following BCG therapy. These
338 observations align with current literature highlighting the importance of CD79a+ B cells in
339 driving tumor progression and fostering resistance to BCG therapy, particularly within the
340 stromal milieu [21].

341 A higher stromal B cell density and a positive correlation between densities of CD79a+ B cells,
342 M2-like macrophages, CD103+ cells, PD-1 immune checkpoint expression, compared to that of
343 the epithelial compartment, is indicative of chronic inflammation and potential exhaustion
344 within or outside of either stromal immune cell aggregates or bladder mucosa associated
345 lymphoid tissue referred to as tertiary lymphoid structures (TLSs). Mucosa associated TLSs
346 evolve as a result of chronic inflammation such as carcinogen exposure or persistent antigenic
347 stimuli including recurrent urinary tract infection or autoimmune mediated Hunner's lesion
348 interstitial cystitis [25]. Supporting this, our previous report demonstrated the compounding

349 effects of aging and chronic carcinogenesis associated inflammation on increased B cell
350 recruitment and TLS formation in the urinary bladder [26, 27]. We also showed the higher
351 expression of multiple immune exhaustion associated proteins within TLSs and their peri-
352 tumoral location associated with higher stage and poor response to BCG [26, 28]. A bladder
353 tumor associated chronic inflammatory state also suggests an exhausted pre-BCG host immune
354 system. Consequent to such systemic immune exhaustion, exposure to BCG bacteria at weekly
355 intervals during the induction phase of treatment potentially intensifies the chronic systemic
356 inflammatory state, specifically in patients with higher stromal B cell profiles in their pre-BCG
357 tumors. This is supported by a recent study conducted by Strangaard *et al.,* [20] which
358 examined pre- and post- BCG paired tumor samples and showed T cell exhaustion as the factor
359 underlying a BCG unresponsive disease. Overall, these findings suggest that in a subset of
360 patients who do not benefit from BCG, signatures of innate and adaptive immune exhaustion
361 within the pre-BCG tumor immune profiles could inform patient selection for
362 immunomodulatory BCG treatment.

363 Most recently, de Jong *et al.*, reported the presence of three BCG response subtypes (BRS1,
364 BRS2, and BRS3) of pre-treatment tumors that show a distinct association with progression of
365 NMIBC to muscle invasive disease [21]. Specifically, in this study based on bulk RNA-sequencing
366 of tumors, the BRS3 subtype enriched with immune gene signatures was shown to associate
367 with poor outcomes following BCG treatment. Tumors with a BRS3 subtype (increased
368 expression of genes associated with B cell, M1/M2 macrophage, CD8+ T cell, $T_{reg}$ function and
369 immune exhaustion) exhibited the most aggressive behavior and early progression. Notably,
370 luminal subtype tumors that are known to exhibit a low immune infiltration profile, were not
371 enriched for a BRS3 gene signature. Unsurprisingly, the post-BCG recurrent tumors also carried
372 the BRS3 phenotype and a basal tumor subtype [21]. In the current study, we used the pan B
373 cell marker - CD79a, to identify tumor infiltrating B cells. Evaluation of bulk RNA-Seq profiles
374 from the publicly available tumor transcriptomic profiles of 283 patients generated by de Jong
375 *et al.,* validated our findings on the increased expression of *CD79A* and *CD163* transcripts in
376 tumors from patients who experienced early progression to muscle invasive disease following
377 BCG therapy.

378 Our counterintuitive findings showing inverse correlations between higher density of cytotoxic
379 T cells and poor response to BCG immunotherapy, are also in alignment with previous literature
380 suggesting the development of adaptive immune resistance following treatment in BCG non-
381 responders [19, 21]. Previous studies have highlighted the involvement of regulatory B cell
382 subsets in fostering an immunosuppressive environment conducive to immune evasion and
383 tumor progression [29-31]. Remarkably, our study corroborates these prior findings,
384 establishing a positive correlation between CD79a+ B cells and CD163+ M2-like macrophages,
385 CD8+ Ki67+ proliferating cytotoxic T-cells, and PD-1 expression within the stromal compartment
386 of BCG-refractory patients.

387 The notable correlation between CD79a+ B-cells, CD8+ T cells and the PD-1 immune checkpoint
388 protein suggests a potential regulatory role exerted by immune checkpoint mechanisms in
389 modulating the functional activity of cytotoxic T cells in response to BCG therapy. Similarly, the
390 presence of CD8+ T cells and CD103+ cells implies an actively mounting immune response
391 against the tumor. However, their correlation with shorter RFS strongly suggests the possibility
392 of dysfunction or exhaustion, potentially arising from chronic antigen exposure or inhibitory
393 signals from other immune cell subsets. Immune cells expressing the $\alpha_E$ integrin CD103 (mainly
394 $T_{RM}$ cells) are widely distributed across mucosal surfaces [32]. In this study we did not use a T
395 cell phenotypic marker to define CD103+ cell, however, their significantly high correlation with
396 CD8+ cells and previous reports confirming the T cell specific intra-tumoral expression pattern
397 of CD103 and the chronic nature of the disease, is suggestive of their $T_{RM}$ phenotype [33, 34].
398 Indeed, the expression of CD103 has been reported on multiple cell types (Tregs, tissue resident
399 memory T cells) within the stromal compartment across various cancer types [35]. Future
400 studies should further characterize their effector memory and central memory functional
401 states.

402 Overall, these findings from multiple independent cohorts confirm that spatial organization and
403 density of B cells within the pre-BCG TIME could be developed into a robust clinically feasible
404 assay for application on TURBT specimens prior to initiation of BCG treatment.

405 An important and novel finding from our study is the significantly worse RFS and PFS in BCG
406 treated female patients with high stromal and intra-epithelial B cell density compared to that of
407 males. As reported by us and others, the physiologically higher B cell frequency in females
408 compared to that of males is likely a key factor underlying the higher degree of their trafficking
409 to the bladder TIME upon chronic antigenic stimulation. Previously, we have reported a
410 significantly shorter PFS in females based on evaluation of two large independent cohorts of
411 patients with NMIBC. We also showed that irrespective of the treatment type, a higher pre-
412 treatment intra-tumoral B cell density is associated with early RFS and PFS in patients with
413 NMIBC [18].

414 While these findings indicate that B cell proportions increase with disease progression and due
415 to the immune stimulatory effects of BCG bacteria, we speculate that upon treatment with
416 cytotoxic chemotherapy such as gemcitabine-docetaxel chemotherapy or immune checkpoint
417 inhibition, such responses may lead to a favorable response via immunogenic cell death
418 mediated events. Such associations have been reported in other cancers and in muscle invasive
419 bladder cancer, where higher pre-treatment B cell density associated with positive outcomes
420 following treatment [36-38]. Finally, in this study, we observed a significant association
421 between increased density of CDK5+ PDL-1+ cells indicative of an aggressive cancer cell
422 phenotype and shorter PFS. Constitutive expression of PD-L1 on cancer cells could result from
423 mutations in DNA damage repair genes or could be induced via the phenomenon of adaptive
424 immune resistance during disease progression [39]. While the mutational profiles of tumors
425 used in our study were not available, previous studies have reported an enrichment of DNA
426 damage repair gene mutations in high-grade NMIBC tumors [40, 41].

427 This study is not without limitations. We acknowledge that tumor cores of 0.6 - 1 mm diameter
428 in a TMA do not capture the heterogeneity within the larger tumor landscape. Recently,
429 Lindskrog *et al.*, [23] reported the presence of multiple tumor subtypes within a single tumor
430 specimen. This finding supports a potential caveat of TMA based studies and the need for
431 surveying whole tumor sections to derive a comprehensive spatial organization. However, with
432 regard to our previous report confirming stromal B cell infiltration profiles, and TLSs in whole
433 tumor sections of BCG non-responders, we posit that a careful selection of tissue cores

434 capturing tumor invasive margins is required for larger cohort-based biomarker studies. A
435 deeper characterization of the B cell subsets and their cellular neighborhoods using whole
436 tumor sections is also needed to gain further insights into their antigen presenting and/or
437 antibody producing functions. Finally, exploration of the finer spatial relationships between the
438 several immune cell populations and tumor invasive margins within pre- and post-BCG
439 treatment tumors is critical to determine if the localization of specific cellular phenotypes
440 associate with BCG outcome.

441 To conclude, the findings presented in this study advance the current understanding of the
442 immune landscape characterizing the NMIBC microenvironment and its association with patient
443 responses to BCG immunotherapy. Ultimately, these findings have implications not only for the
444 development of novel therapeutic strategies targeting B cell specific exhaustion but also to
445 inform approaches for precise sequencing of drugs targeting the immune checkpoint pathways
446 to improve the efficacy of treatments for NMIBC. The results also contribute to a growing body
447 of literature on sex differences in the immune cell landscape and the importance of sex
448 considerations in BCG immunotherapy and the need for a sex-disaggregated data analyses
449 approach in biomarker studies to address the interpretations associated with inconsistent
450 findings across different cohorts. Given the advent of newer immunotherapies as well as
451 gemcitabine-docetaxel chemotherapy in the BCG naïve setting, early identification of patients
452 who may not benefit from BCG, using information from pre-treatment immune landscape, will
453 allow precise incorporation of newer therapeutics in NMIBC.

454

455 **Conflict of interest statement**

456 All authors have no conflicts of interest to disclose.

457 **Author contributions and acknowledgements**

458 MK conceptualized the overall study and contributed to study design, manuscript writing and
459 revision. DRS and BR contributed to the study design. SC performed manual validation of mIF
460 staining and automated scoring. BR performed all data analysis relating to the KHSC cohort and

461 contributed to manuscript writing and revision. PY, SR and KP contributed to manuscript
462 writing and revision. KS, HG and AG performed additional analysis included in this study, such
463 as analysis for the independent validation cohort and subtyping and contributed to manuscript
464 writing and reviewing. CJ and DMB provided the KHSC tissue cohort and associated clinical data.
465 KT guided all data analysis. DRS and CJ helped with clinical classifications of BCG treated patient
466 specimens. All authors reviewed the manuscript. PY is supported by Robert Wilson Fellowship
467 for PhD training. This study was supported by research operating grants from Bladder Cancer
468 Canada (MK, DRS and DMB), Cancer Research Society (MK, DRS and DMB), Ontario Institute for
469 Cancer Research/Ontario Molecular Pathology Research Network (DMB); Ontario Ministry of
470 Research Innovation and Science: Early Researcher Award and Canada Foundation for
471 Innovation (MK). We thank Shakeel Virk at the QLMP for his assistance with imaging and Halo
472 software and Katy Milne at BC Cancer Agency's Molecular and Cellular Immunology Core for
473 immunofluorescence staining of TMAs.

474 **References**


475 1. Koti, M., et al., *Sex Differences in Bladder Cancer Immunobiology and Outcomes: A Collaborative*
476 *Review with Implications for Treatment.* Eur Urol Oncol, 2020.
477 2. Uhlig, A., et al., *Gender-specific Differences in Recurrence of Non–muscle-invasive Bladder*
478 *Cancer: A Systematic Review and Meta-analysis.* European Urology Focus, 2018. **4**(6): p. 924-
479 936.
480 3. Marks, P., et al., *Female with bladder cancer: what and why is there a difference?* Transl Androl
481 Urol, 2016. **5**(5): p. 668-682.
482 4. Krimphove, M.J., et al., *Sex-specific Differences in the Quality of Treatment of Muscle-invasive*
483 *Bladder Cancer Do Not Explain the Overall Survival Discrepancy.* Eur Urol Focus, 2019.
484 5. Roumiguie, M., et al., *International Bladder Cancer Group Consensus Statement on Clinical Trial*
485 *Design for Patients with Bacillus Calmette-Guerin-exposed High-risk Non-muscle-invasive*
486 *Bladder Cancer.* Eur Urol, 2021.
487 6. Lobo, N., et al., *Updated European Association of Urology (EAU) Prognostic Factor Risk Groups*
488 *Overestimate the Risk of Progression in Patients with Non-muscle-invasive Bladder Cancer*
489 *Treated with Bacillus Calmette-Guerin.* Eur Urol Oncol, 2021.
490 7. Matulay, J.T., et al., *Contemporary Outcomes of Patients with Nonmuscle-Invasive Bladder*
491 *Cancer Treated with bacillus Calmette-Guerin: Implications for Clinical Trial Design.* J Urol, 2021.
492 **205**(6): p. 1612-1621.
493 8. Babjuk, M., et al., *European Association of Urology Guidelines on Non-muscle-invasive Bladder*
494 *Cancer (Ta, T1, and Carcinoma in Situ).* Eur Urol, 2022. **81**(1): p. 75-94.
495 9. Kamat, A.M., et al., *Definitions, End Points, and Clinical Trial Designs for Bladder Cancer:*
496 *Recommendations From the Society for Immunotherapy of Cancer and the International Bladder*
497 *Cancer Group.* J Clin Oncol, 2023: p. JCO2300307.
498 10. Goldberg, I.P., et al., *Pharmacologic Therapies for Non-Muscle Invasive Bladder Cancer: Current*
499 *and Future Treatments.* Arch Pharmacol Ther, 2022. **4**(1): p. 13-22.
500 11. Koti, M., et al., *Adaptive Immunity in Genitourinary Cancers.* Eur Urol Oncol, 2023.
501 12. Nazmifar, M., et al., *Clinical and Preclinical Therapies for Bladder Cancer Following Bacillus*
502 *Calmette-Guerin Failure.* J Urol, 2023. **209**(1): p. 32-48.
503 13. Packiam, V.T., et al., *The current landscape of salvage therapies for patients with bacillus*
504 *Calmette-Guerin unresponsive nonmuscle invasive bladder cancer.* Curr Opin Urol, 2021. **31**(3):
505 p. 178-187.
506 14. Balar, A.V., et al., *Pembrolizumab monotherapy for the treatment of high-risk non-muscle-*
507 *invasive bladder cancer unresponsive to BCG (KEYNOTE-057): an open-label, single-arm,*
508 *multicentre, phase 2 study.* Lancet Oncol, 2021. **22**(7): p. 919-930.
509 15. Flaig, T.W., et al., *NCCN Guidelines(R) Insights: Bladder Cancer, Version 2.2022.* J Natl Compr
510 Canc Netw, 2022. **20**(8): p. 866-878.
511 16. Jiang, Y., et al., *Non-invasive tumor microenvironment evaluation and treatment response*
512 *prediction in gastric cancer using deep learning radiomics.* Cell Rep Med, 2023. **4**(8): p. 101146.
513 17. Goto, W., et al., *Predictive value of improvement in the immune tumour microenvironment in*
514 *patients with breast cancer treated with neoadjuvant chemotherapy.* ESMO Open, 2018. **3**(6): p.
515 e000305.
516 18. Chenard, S., et al., *Sexual Dimorphism in Outcomes of Non-muscle-invasive Bladder Cancer: A*
517 *Role of CD163+ Macrophages, B cells, and PD-L1 Immune Checkpoint.* Eur Urol Open Sci, 2021.
518 **29**: p. 50-58.

519 19. Kates, M., et al., *Adaptive Immune Resistance to Intravesical BCG in Non-Muscle Invasive Bladder*
520 *Cancer: Implications for Prospective BCG-Unresponsive Trials.* Clin Cancer Res, 2020. **26**(4): p.
521 882-891.
522 20. Strandgaard, T., et al., *Elevated T-cell Exhaustion and Urinary Tumor DNA Levels Are Associated*
523 *with Bacillus Calmette-Guerin Failure in Patients with Non-muscle-invasive Bladder Cancer.* Eur
524 Urol, 2022. **82**(6): p. 646-656.
525 21. de Jong, F.C., et al., *Non-muscle-invasive bladder cancer molecular subtypes predict differential*
526 *response to intravesical Bacillus Calmette-Guerin.* Sci Transl Med, 2023. **15**(697): p. eabn4118.
527 22. Newman, T.B. and W.S. Browner, *In defense of standardized regression coefficients.*
528 Epidemiology, 1991. **2**(5): p. 383-6.
529 23. Lindskrog, S.V., et al., *Single-nucleus and Spatially Resolved Intratumor Subtype Heterogeneity in*
530 *Bladder Cancer.* Eur Urol Open Sci, 2023. **51**: p. 78-88.
531 24. Sun, M., et al., *Infiltration and Polarization of Tumor-associated Macrophages Predict Prognosis*
532 *and Therapeutic Benefit in Muscle-Invasive Bladder Cancer.* Cancer Immunol Immunother, 2022.
533 **71**(6): p. 1497-1506.
534 25. Koti, M. and D.R. Siemens, *The Evolving Landscape of Bladder Tertiary Lymphoid Structures.* J
535 Urol, 2023. **210**(1): p. 3-4.
536 26. Koti, M., et al., *Tertiary Lymphoid Structures Associate with Tumour Stage in Urothelial Bladder*
537 *Cancer.* Bladder Cancer, 2017. **3**(4): p. 259-267.
538 27. Hamade, A., et al., *Sex differences in the aging murine urinary bladder and influence on the*
539 *tumor immune microenvironment of a carcinogen-induced model of bladder cancer.* Biol Sex
540 Differ, 2022. **13**(1): p. 19.
541 28. Priyanka Yolmo, S.R., Stephen Chenard, Gwenaëlle Conseil, Danielle Jenkins, Kartik Sachdeva,
542 Isaac Emon, Jake Hamilton, Minqi Xu, Manu Rangachari, Eva Michaud, Jose Mansure, Wassim
543 Kassouf, David M. Berman, D. Robert Siemens, Madhuri Kot, *Atypical B cells mediate poor*
544 *response to Bacillus Calmette Guérin immunotherapy in non-muscle invasive bladder cancer.*
545 bioRxiv, 2022(522127).
546 29. Zirakzadeh, A.A., et al., *Tumour-associated B cells in urothelial urinary bladder cancer.* Scand J
547 Immunol, 2020. **91**(2): p. e12830.
548 30. Schwartz, M., Y. Zhang, and J.D. Rosenblatt, *B cell regulation of the anti-tumor response and role*
549 *in carcinogenesis.* J Immunother Cancer, 2016. **4**: p. 40.
550 31. Fehres, C.M., et al., *APRIL Induces a Novel Subset of IgA(+) Regulatory B Cells That Suppress*
551 *Inflammation via Expression of IL-10 and PD-L1.* Front Immunol, 2019. **10**: p. 1368.
552 32. Sheridan, B.S. and L. Lefrancois, *Regional and mucosal memory T cells.* Nat Immunol, 2011.
553 **12**(6): p. 485-91.
554 33. Wang, Z.Q., et al., *CD103 and Intratumoral Immune Response in Breast Cancer.* Clin Cancer Res,
555 2016. **22**(24): p. 6290-6297.
556 34. Webb, J.R., K. Milne, and B.H. Nelson, *Location, location, location: CD103 demarcates*
557 *intraepithelial, prognostically favorable CD8(+) tumor-infiltrating lymphocytes in ovarian cancer.*
558 Oncoimmunology, 2014. **3**: p. e27668.
559 35. Kim, Y., Y. Shin, and G.H. Kang, *Prognostic significance of CD103+ immune cells in solid tumor: a*
560 *systemic review and meta-analysis.* Sci Rep, 2019. **9**(1): p. 3808.
561 36. Wahlin, S., et al., *Clinical impact of T cells, B cells and the PD-1/PD-L1 pathway in muscle invasive*
562 *bladder cancer: a comparative study of transurethral resection and cystectomy specimens.*
563 Oncoimmunology, 2019. **8**(11): p. e1644108.
564 37. Fu, H., et al., *Identification and Validation of Stromal Immunotype Predict Survival and Benefit*
565 *from Adjuvant Chemotherapy in Patients with Muscle-Invasive Bladder Cancer.* Clin Cancer Res,
566 2018. **24**(13): p. 3069-3078.

567 38. Vidotto, T., et al., *DNA damage repair gene mutations and their association with tumor immune*
568 *regulatory gene expression in muscle invasive bladder cancer subtypes.* J Immunother Cancer,
569 2019. **7**(1): p. 148.
570 39. Miao, Y., et al., *Adaptive Immune Resistance Emerges from Tumor-Initiating Stem Cells.* Cell,
571 2019. **177**(5): p. 1172-1186 e14.
572 40. Pietzak, E.J., et al., *Inherited Germline Cancer Susceptibility Gene Variants in Individuals with*
573 *Non-Muscle-Invasive Bladder Cancer.* Clin Cancer Res, 2022. **28**(19): p. 4267-4277.
574 41. Lindskrog, S.V., et al., *An integrated multi-omics analysis identifies prognostic molecular*
575 *subtypes of non-muscle-invasive bladder cancer.* Nat Commun, 2021. **12**(1): p. 2301.

576

577

578 ***Table 1: Categories of BCG therapy response.***

| **BCG-refractory tumour (as per standard definitions)[8]** |
|---|
| 1. If T1 G3/HG tumour is present at 3 mo. |
| 2. If TaG3/HG tumour is present after 3 months and/or at 6 mo., after either re-induction or first course of maintenance. |
| 3. If CIS (without concomitant papillary tumour) is present at 3 mo. and persists at 6 mo. after either reinduction or a first course of maintenance. For patients with CIS present at 3 mo., an additional BCG course can achieve a complete response in >50% of cases. |
| 4. If HG tumour appears during BCG maintenance therapy. |
| **BCG responsive** |
| 1. No HG tumour recurrence within 2 years following initial adequate BCG induction. |

579

580

581 ***Table 2: Patient cohort clinical characteristics.***

| | BCG Responsive (N=124) | BCG Refractory (N=37) | BCG relapsing (N=12) | Overall (N=173) |
|---|---|---|---|---|
| **Age** | | | | |
| Mean | 71.5 | 68.3 | 72.3 | 70.8 |
| Median | 71.5 | 69.0 | 73.0 | 71.0 |
| Range | 35-93 | 45-85 | 62-82 | 35-93 |
| **Sex** | | | | |
| Male | 102 (82.3%) | 27 (73.0%) | 10 (83.3%) | 139 (80.3%) |
| Female | 22 (17.7%) | 10 (27.0%) | 2 (16.7%) | 34 (19.7%) |
| **AUA Risk Score** | | | | |
| High | 74 (59.7%) | 36 (97.3%) | 12 (100.0%) | 122 (70.5%) |
| Intermediate | 41 (33.1%) | 1 (2.7%) | 0 (0%) | 42 (24.3%) |
| Low | 9 (7.3%) | 0 (0%) | 0 (0%) | 9 (5.2%) |
| **Diagnosis TURBT Stage and Grade** | | | | |
| CIS | 11 (8.9%) | 1 (2.7%) | 1 (8.3%) | 13 (7.5%) |
| PUNLMP | 1 (0.8%) | 0 (0%) | 0 (0%) | 1 (0.6%) |
| T1HG | 32 (25.8%) | 15 (40.5%) | 4 (33.3%) | 51 (29.5%) |
| TaHG | 51 (41.1%) | 17 (45.9%) | 5 (41.7%) | 73 (42.2%) |
| TaLG | 29 (23.4%) | 2 (5.4%) | 2 (16.7%) | 33 (19.1%) |
| Unknown | 0 (0%) | 2 (5.4%) | 0 (0%) | 2 (1.2%) |
| **Time to Follow-up** | | | | |
| Median time to follow-up (months) | 53.4 | 57.9 | 65.4 | 54.3 |
| **BCG Adequacy** | | | | |
| Adequate BCG | 47 (37.9%) | 23 (62.2%) | 11 (91.7%) | 81 (46.8%) |
| Induction only | 77 (62.1%) | 14 (37.8%) | 1 (8.3%) | 92 (53.2%) |
| **Subtype** | | | | |
| Genomically Unstable | 13 (10.3%) | 3 (7.7%) | 1 (8.3%) | 17 (9.6%) |
| URO-KRT5+ | 11 (8.7%) | 2 (5.1%) | 2 (16.7%) | 15 (8.5%) |
| Urothelial-like | 9 (7.1%) | 7 (17.9%) | 1 (8.3%) | 17 (9.6%) |
| Basal | 1 (0.8%) | 1 (2.6%) | 0 (0.0%) | 2 (1.1%) |
| Not Subtyped | 92 (73.0%) | 26 (66.7%) | 8 (66.7%) | 126 |
| **Subtype Grade** | | | | |
| 1 | 27 (21.4%) | 7 (17.9%) | 2 (16.7%) | 36 (20.3%) |
| 2 | 7 (5.6%) | 6 (15.4%) | 2 (16.7%) | 15 (8.5%) |
| Not Subtyped | 92 (73.0%) | 26 (66.7%) | 8 (66.7%) | 126 |

582

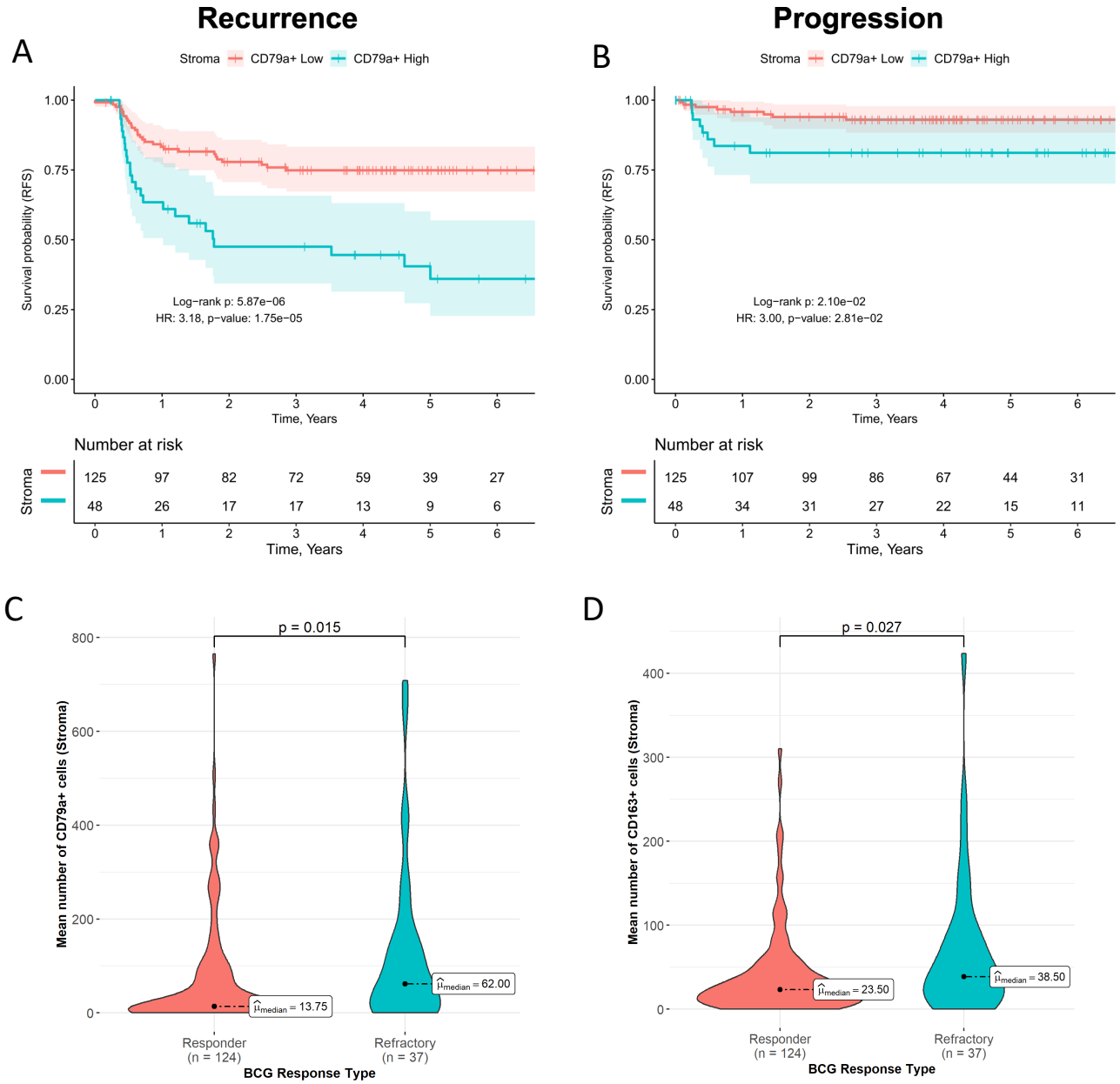


**Figure 1. High intra-tumoral CD79a+ B cell density associates with early recurrence and progression post BCG immunotherapy. A)** Patients with high stromal CD79a+ B cell density have significantly shorter RFS compared to patients with low density (Log-rank p=5.83e-6, IRR=0.29, HR=3.18, p=1.75e-5). **B)** Patients with high stromal CD79a+ B cell density have significantly shorter PFS compared to patients with low density (Log-rank p=2.07e-2, IRR=0.32, HR=3.00, p=2.8e-2), **C)** BCG refractory patients have significantly higher stromal CD79a+ cell density compared to BCG responders ($W_{Mann\text{-}Whitney}$=1744.5, p=0.027), and **D)** BCG refractory patients have significantly higher stromal CD163 cell density compared to BCG responders ($W_{Mann\text{-}Whitney}$=1688.00, p=0.015).

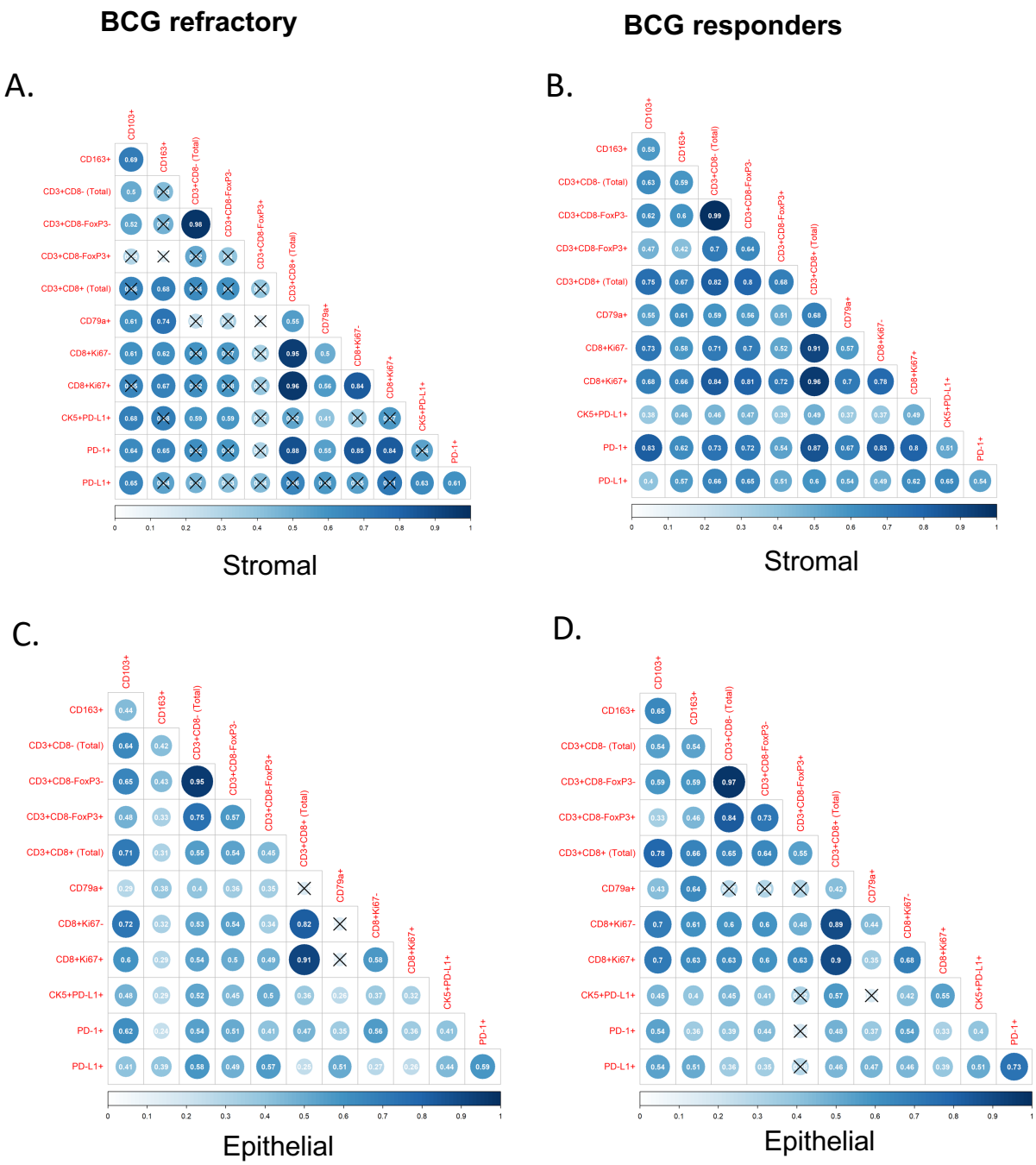


**Figure 2. Stromal CD79a+ B cells are strongly correlated with CD163+ M2-like macrophages, CD8+ cytotoxic T cells, CD103+ cells and PD-1 immune checkpoint expression.** Spearman correlation plot for immune cell populations in the stromal (A and B) and epithelial (C and D) compartments of tumors from BCG responders and refractory. Correlation plots showing the correlations between immune cells in tumor from patients categorized as BCG refractory and responders.

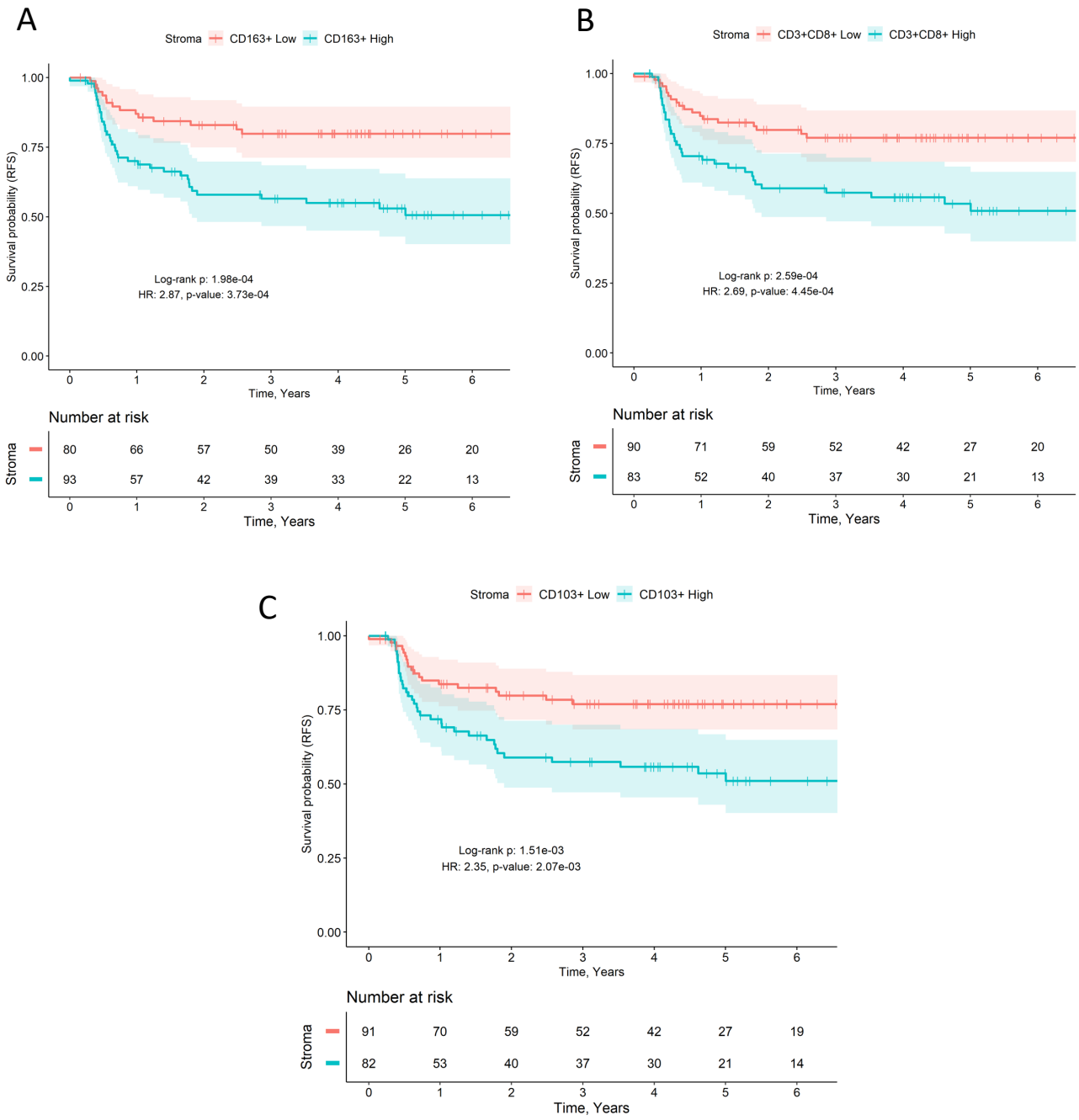


**Figure 3. High tumor infiltrating M2-like macrophage, CD8+ and CD103+ T cell density associates with early recurrence post BCG immunotherapy. A)** Patients with high stromal CD163+ macrophage density have significantly worse RFS compared to patients with low density. Log-rank p=1.98e-6, IRR=0.31, HR=2.87, p=3.73e-4. **B)** Patients with high stromal CD3+CD8+ cell density have significantly worse RFS compared to patients with low density. Log-rank p=2.59e-4, IRR=0.34, HR=2.69, p=4.45e-2. **C)** Patients with high stromal CD103+ cell density have significantly worse RFS compared to patients with low density. Log-rank p=1.51e-3, IRR=0.40, HR=2.35, p=2.07e-3

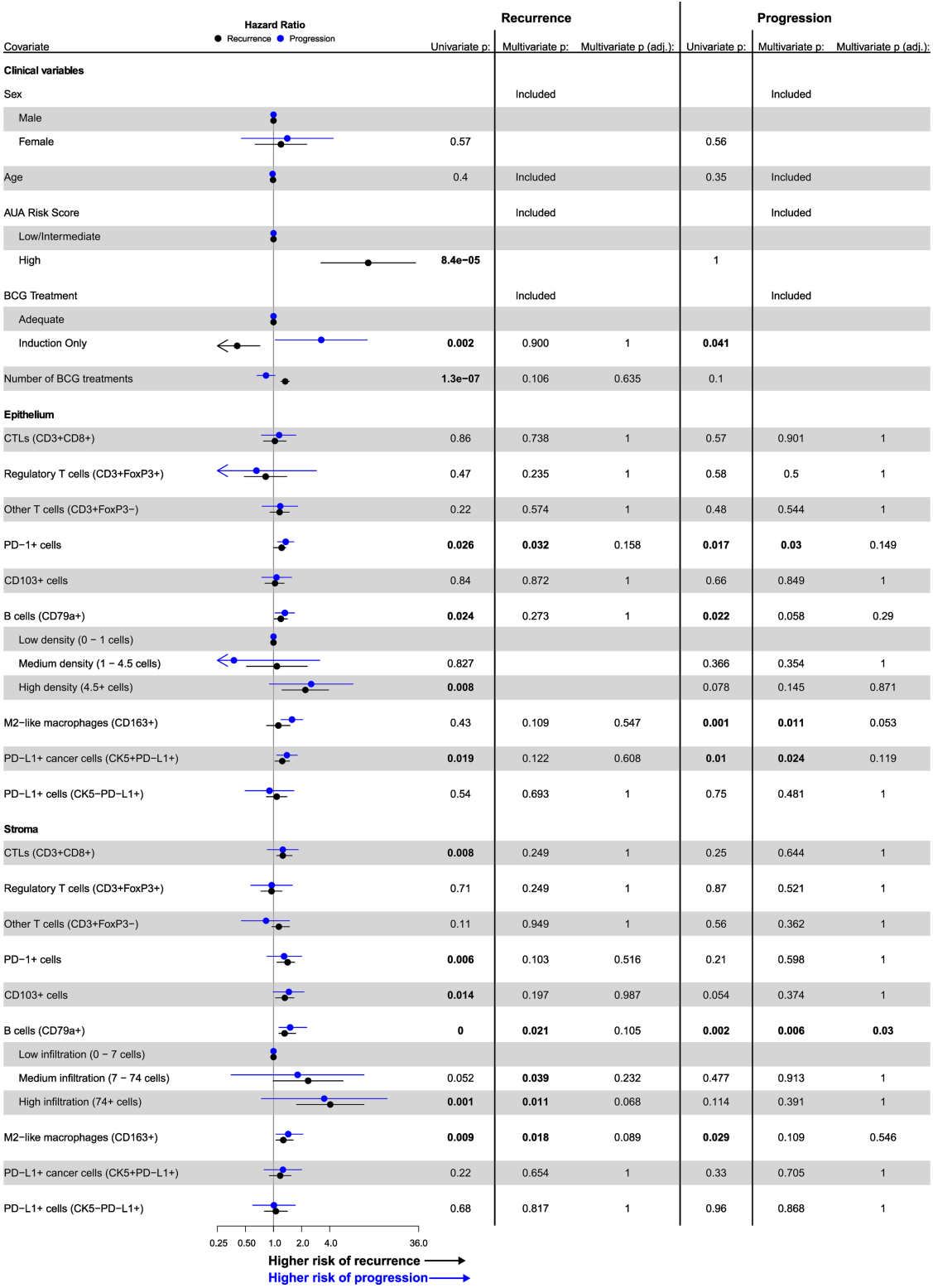


**Figure 4. Forest plots demonstrating patient demographics and immune markers with clinical outcomes post BCG immunotherapy.** Forest plot based showing univariate Cox Proportional Hazards (CPH) regression analyses, with recurrence highlighted in black and progression in blue. Dots represent hazard ratios and lines represent the 95% confidence intervals. Hazard ratios for immune cell types are displayed graphically in terms of risk per standard deviation (σ) increment in cell infiltration. Multivariable CPH regression analyses were performed for each immune phenotype separately, including sex, age, AUA risk score, and amount of BCG treatment received after the analyzed tumor. P values were calculated using the Wald test, and multivariable p values were adjusted using the Bonferroni correction.